ChemComm

COMMUNICATION

View Article Online
View Journal

Cite this: DOI: 10.1039/d3cc05369e

Received 31st October 2023,
Accepted 17th December 2023

DOI: 10.1039/d3cc05369e

rsc.li/chemcomm

Contrasting reactivity of B–Cl and B–H bonds at [Ni(IMes)$_2$] to form unsupported Ni-boryls†

Gabrielle Audsley,[a] Ambre Carpentier,[b] Anne-Frédérique Pécharman,[c] James Wright,[a] Thomas M. Roseveare,[d] Ewan R. Clark,[e] Stuart A. Macgregor*[b] and Ian M. Riddlestone*[a]

[Ni(IMes)$_2$] reacts with chloroboranes *via* oxidative addition to form rare unsupported Ni-boryls. In contrast, the oxidative addition of hydridoboranes is not observed and products from competing reaction pathways are identified. Computational studies relate these differences to the mechanism of oxidative addition: B–Cl activation proceeds *via* nucleophilic displacement of Cl$^-$, while B–H activation would entail high energy concerted bond cleavage.

The transition metal-catalysed borylation of organic substrates is an efficient method for the preparation of organoboronate esters and boronic acids,[1,2] which serve as important substrates for C–C coupling reactions in the synthesis of complex molecules.[3,4] Transition metal-boryls (M-BX$_2$)[5,6] are key intermediates in these borylation reactions[7–10] and whilst many of these reactions rely on precious metals, the economic and environmental credentials of the 3*d* metals have seen a focus on their applications in borylation catalysis.[11] There have been a number of reports of nickel-catalysed borylations[12] but despite Ni-boryls often being proposed as intermediates in these cycles, examples of characterised Ni-boryls remain rare.[13–19] This reflects both the reactivity of the Ni–BX$_2$ bond and the challenges associated with its formation.

The formation of Pt-boryls *via* the oxidative addition of B–B and B–X bonds (X = halogen or H) is well established[20–24] and B–halogen oxidative addition has also been used for the formation of Pd-boryls.[25–28] In contrast, examples of Ni-boryls formed by oxidative addition are limited to the bis-boryls *cis*-[Ni(^{i}Pr$_2$Im^{Me})$_2$(B(OR)$_2$)$_2$] (^{i}Pr$_2$Im^{Me} = 1,3-diisopropyl-imidazolin-2-ylidene; OR = ½ catecholato, pinacolato or ethylene glycolato) formed from the reaction between the corresponding diboranes and [Ni$_2$(^{i}Pr$_2$Im^{Me})$_4$(μ-(η^2:η^2)-COD)]/[Ni(^{i}Pr$_2$Im^{Me})$_2$(η^4-COD)] (Fig. 1).[17] However, detailed analysis of the bonding in these bis-boryls shows oxidative addition to be incomplete with the structure lying between a Ni(II) bis-boryl and a non-classical Ni(0) diborane(4) complex. Other examples of Ni-boryls formed *via* oxidative processes are the [(^{Ph}PBP)Ni]$_2$ Ni(I) dimer reported by Peters,[14] resulting from one electron reactivity between the ^{Ph}PBP(H) pincer ligand and [Ni(COD)$_2$], and the related [(^{Ph}PBP)NiCl] and chelating phosphine/boryl formed by oxidative dehydrochloroborylation reported by Nozaki (Fig. 1).[19] Boryl formation *via* simple oxidative addition of a B–X bond (X = halogen or H) at a Ni(0) centre, in a manner analogous to precious metals, has not been reported.

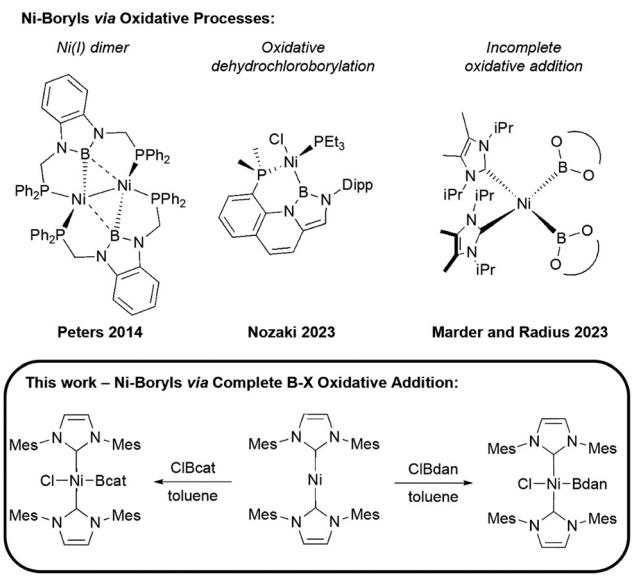

Fig. 1 (top) Examples of Ni-boryls formed by oxidative processes; (bottom) Ni-boryl synthesis *via* oxidative addition (cat = catecholato; dan = 1,8-diaminonaphthalato).

[a] School of Chemistry and Chemical Engineering, University of Surrey, Guildford GU2 7XH, UK. E-mail: i.riddlestone@surrey.ac.uk
[b] Institute of Chemical Sciences, Heriot-Watt University, Edinburgh, EH14 4AS, UK. E-mail: S.A.Macgregor@hw.ac.uk
[c] Department of Chemistry, University of Bath, Claverton Down, Bath, BA2 7AY, UK
[d] Department of Chemistry, University of Sheffield, S3 7HF, UK
[e] School of Physical Sciences, University of Kent, Canterbury, CT2 7NH, UK

† Electronic supplementary information (ESI) available. CCDC 2304313–2304318. For ESI and crystallographic data in CIF or other electronic format see DOI: https://doi.org/10.1039/d3cc05369e

The reactivity of Ni-boryls is receiving increased attention and the nucleophilicity of the boryl ligand has been demonstrated by the borylation of bromobenzene by [(PNP)Ni(Bcat)][13] and the reactivity of *cis*-[Ni(^{i}Pr$_2$Im^{Me})$_2$(Bcat)$_2$] towards alkyl halides.[18] Incorporation of the boryl into a PBP-pincer ligand has allowed exploitation of its strong σ-donor and potential π-acceptor capabilities for the activation of H_2,[15,16] dimerization of ethylene[29] and cleavage of CO_2.[30] With increased interest in Ni-boryls and their applications in bond activation and catalysis we now report the ready formation of stable unsupported Ni-boryls by the oxidative addition of the B–Cl bond at the Ni(0) precursor [Ni(IMes)$_2$]. Interestingly, the analogous oxidative addition of B–H bonds does not occur, and this stark difference between B–H and B–Cl activation is explored computationally. This further highlights the complexity of the oxidative addition of catalytically relevant substrates at Ni(0) precursors.[31]

The addition of a toluene solution of either ClBcat or ClBdan to a toluene solution of [Ni(IMes)$_2$], **1**, results in a progressive colour change from the dark purple colour of the Ni(0) precursor to a dark yellow or orange solution respectively. This colour change is accompanied by the loss of the ^{11}B NMR resonance associated with the haloborane and the appearance of a new broad resonance at δ_B = 37.3 or 41.6 ppm for the corresponding products of oxidative addition *trans*-[Ni(IMes)$_2$(Bcat)Cl] (**2**) and *trans*-[Ni(IMes)$_2$(Bdan)Cl] (**3**) respectively. Crystallisation through the storage of saturated solutions of **2** and **3** at −20 °C allowed for their characterisation by single crystal X-ray diffraction confirming their identity as new unsupported Ni-boryls (Fig. 2).

The Ni–B bond distances of *trans*-[Ni(IMes)$_2$(Bcat)Cl] (**2**) and *trans*-[Ni(IMes)$_2$(Bdan)Cl] (**3**) are 1.908(4) Å and 1.911(3) Å respectively. The ligand *trans* to the boryl clearly influences the Ni–B bond distance as those observed for **2** and **3** are similar to that of [(PNP)Ni(Bcat)] (1.9091(18) Å),[13] in which the boryl ligand is *trans* to an amide, but within the range defined by being *trans* to another boryl [(PBP)Ni(Bcat)] (2.015(2) Å)[16] and the heavier halogens in *trans*-[(^{i}Pr$_2$Im^{Me})$_2$Ni(Bcat)X] (X = Br, 1.872(4) Å; X = I, 1.864(4) Å).[18] Comparison to the Ni–B bond distances observed in *cis*-[(^{i}Pr$_2$Im^{Me})$_2$Ni(Bcat)$_2$] (1.9231(19) Å and 1.9092(18) Å),[17] for which a B–B interaction is still present and the overall bonding picture is more complex, is also pertinent.

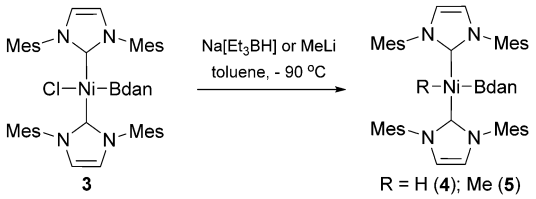

Scheme 1 Reactivity of [Ni(IMes)$_2$(Bdan)Cl] (**3**) with Na[Et$_3$BH] and MeLi.

Characterisation by multinuclear NMR spectroscopy (see ESI†) showed that clean samples of both **2** and **3** are stable in solution for hours at room temperature. However, the isolation of clean material from the preparation of **2** was hampered by the redistribution of the catechol scaffold as has been observed previously.[32–34] Furthermore, **2** was shown to be unstable in the presence of ClBcat with its addition to samples initiating the decomposition of the Ni-boryl and the further redistribution of the catechol ligand (see ESI†). The Bdan scaffold proved to be far more resistant to redistribution providing a cleaner overall reaction and allowing for more facile isolation of the Ni-boryl **3** in up to 79% of clean material.

To establish both if the chloride ligand of **3** could be substituted and whether the hydride-containing species *trans*-[Ni(IMes)$_2$(Bdan)H], the product of oxidative addition of the corresponding hydridoborane, would be a viable target, reactions with Na[Et$_3$BH] and MeLi were undertaken (Scheme 1). Addition of Na[Et$_3$BH] or MeLi to a toluene solution of **3** at low temperature resulted in a shift in the ^{11}B NMR resonance from δ_B = 41.6 ppm to δ_B = 48.1 and 49.3 ppm, consistent with the substitution of the chloride ligand and formation of the new Ni-boryl complexes *trans*-[Ni(IMes)$_2$(Bdan)H] (**4**) and *trans*-[Ni(IMes)$_2$(Bdan)-Me] (**5**). For **5**, filtration followed by removal of the solvent and storage of a concentrated ether solution at −20 °C resulted in the formation of single crystals suitable for X-ray diffraction. The structure of **5** (Fig. 2) confirms the presence of the boryl ligand *trans* to a Me group and substitution of the chloride ligand. Furthermore, the Ni–B bond distance of 1.9688(17) Å is longer than that in **3** (*cf.* 1.911(3) Å), consistent with the greater *trans* influence of the alkyl ligand. Although **5** is thermally unstable in solution (see ESI†), showing significant decomposition in 2 hours at room temperature, it has been fully characterised

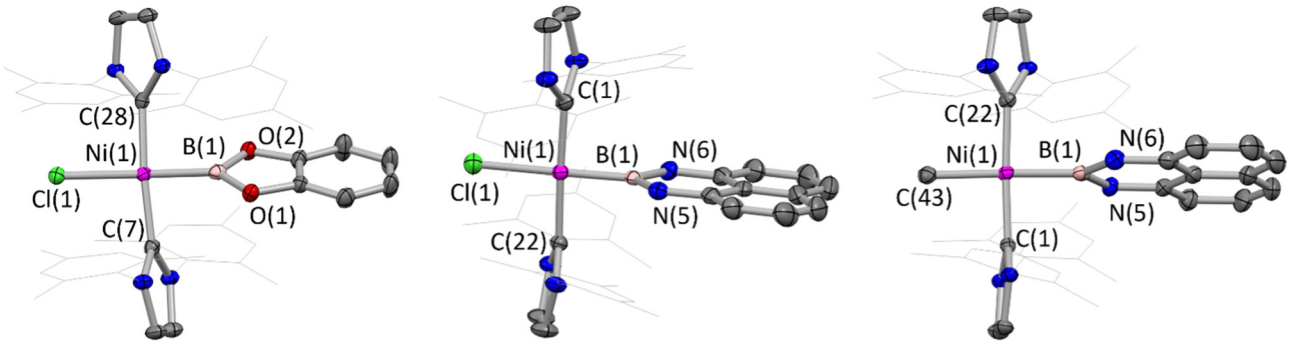

Fig. 2 Molecular structures of **2** (left), **3** (centre) and **5** (right) with thermal ellipsoids at the 50% probability level. Mesityl substituents are shown in wireframe, solvents of crystallisation and hydrogen atoms omitted for clarity.

by multinuclear NMR and elemental analysis. **4** is also thermally unstable but spectroscopic data of isolated material are consistent with its assignment as *trans*-[Ni(IMes)$_2$(Bdan)H] (see ESI†) with the Ni–H resonance readily identified in the ^{1}H NMR spectrum at $\delta_H = -4.62$ ppm.

The spectroscopic characterisation of **4** suggests that oxidative addition of hydridoboranes may also be possible at [Ni(IMes)$_2$], similar to well-established Rh-catalysed hydroboration chemistry.[9,35] However, the reactivity of [Ni(IMes)$_2$] towards the hydridoboranes HBcat and HBdan contrasts strongly to the chloroboranes, with addition of either of these species to a solution of [Ni(IMes)$_2$] in C_6D_6 providing no evidence for the oxidative addition of either B–H bond and formation of the corresponding Ni-boryls. In the case of HBcat, products resulting from competing one electron pathways were identified and the Ni(I)-containing species [Ni(IMes)$_2$][Bcat$_2$] (**6**, see ESI†) and [Ni$_2$(IMes)$_2$][Bcat$_2$] (**7**, see ESI†) were both characterised by single crystal X-ray diffraction. The Ni(I) cation **6** has previously been characterised,[36,37] but the mixed Ni(0)-Ni(I) dimer **7**, in which each IMes ligand binds through the carbenic carbon to one Ni centre and an η^6-arene interaction to the other Ni, has not been reported and is the IMes analogue of [Ni$_2$(IPr)$_2$][OTf] previously reported by Sadighi.[38]

The addition of HBdan to a C_6D_6 solution of [Ni(IMes)$_2$] resulted in a dark reaction mixture from which colourless crystals were formed over 1 week. Characterisation of these by single crystal X-ray diffraction (see ESI†) showed these to be the product of B–N dehydrocoupling between two HBdan molecules with an IMes ligand bound to one of the boron centres. This contrasting reactivity of [Ni(IMes)$_2$] towards both XBcat and XBdan (X = Cl or H) precursors, despite the product of HBdan oxidative addition **4** being prepared *via* an alternative route, indicates a difference in the mechanism of oxidative addition for B–Cl and B–H bonds at [Ni(IMes)$_2$]. This was therefore investigated computationally, focussing on XBdan for which the experimental outcomes are more clearly defined.

The lowest energy computed reaction profile for the reaction of ClBdan at [Ni(IMes)$_2$] is shown in Fig. 3(a). ClBdan initially forms a B-bound adduct, **Int(1-3)1**, at +2.6 kcal mol^{-1} (Ni–B = 2.20 Å). The elongated B–Cl bond (1.94 Å), and displacement of the Cl away from the Ni centre (Ni···Cl = 2.77 Å) set up this species for B–Cl activation *via* nucleophilic displacement. This proceeds *via* **TS(1-3)** with a barrier of only 7.8 kcal mol^{-1} to form ion-pair **Int(1-3)2** featuring a Ni-boryl bond (1.93 Å) and an outer-sphere Cl$^-$ held primarily *via* a Cl$^-$···H–N contact (2.25 Å). Attempts to locate a transition state for concerted oxidative addition were unsuccessful, and generally converged on **TS(1-3)**.[39] Ni–Cl bond formation then gives **3** at −22.5 kcal mol^{-1}. B–Cl activation is therefore very favourable thermodynamically and proceeds with an overall barrier of 10.4 kcal mol^{-1} *via* nucleophilic displacement of Cl$^-$ by [Ni(IMes)$_2$].

In contrast, HBdan is computed to form a σ-borane complex with [Ni(IMes)$_2$] at −4.1 kcal mol^{-1} (Fig. 3(b), **Int(1-4)1**: Ni–H = 1.67 Å; Ni–B = 2.13 Å; B–H = 1.26 Å). A transition state for concerted oxidative addition on the singlet surface, ^{1}**TS(1-4)**, was characterised but was prohibitively high in energy (+56.3 kcal mol^{-1}). The corresponding transition state on the triplet surface proved more stable (^{3}**TS(1-4)**, +32.2 kcal mol^{-1}) and could be accessed *via* spin-crossover MECP1. ^{3}**TS(1-4)** links to ^{3}**Int(1-4)2** at +23.8 kcal mol^{-1} with a 'see-saw' structure, from which isomerisation and spin-crossover *via* MECP2 would form **4** at −8.1 kcal mol^{-1}. Overall, while **4** is a viable target thermodynamically, it is kinetically inaccessible *via* concerted B–H activation as this incurs a prohibitively high energy span of at least 36.3 kcal mol^{-1} *via* ^{3}**TS(1-4)**, and possibly higher if either MECP were to lie above this.

The greater kinetic accessibility of B–Cl over B–H activation primarily reflects the ability of Cl$^-$ to act as a leaving group: nucleophilic displacement is therefore possible with ClBdan whereas concerted B–H cleavage is the only possibility for

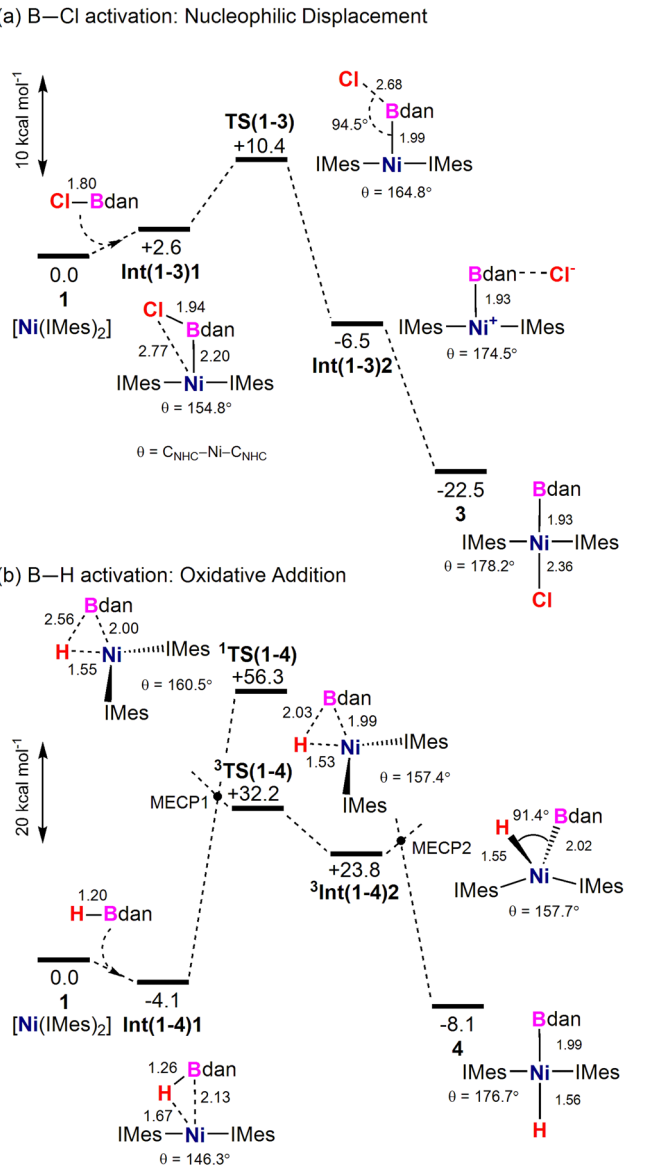

Fig. 3 Computed free energy reaction profiles (kcal mol^{-1}) for (a) B–Cl activation and (b) B–H activation of XBdan at [Ni(IMes)$_2$]. Note the different scales of the two profiles. Minimum energy crossing points (MECPs) between singlet and triplet surfaces were not located. Method: BP86 (Toluene, B3DJ)/Def2TZVP//BP86(Toluene)/6-31G(d,p),SDD (Ni, Cl {ζ = 0.640}).

HBdan.[40] In addition, concerted B–H oxidative addition may be disfavoured by the combination of the bulky IMes and Bdan ligands;[31,36,41,42] in particular in **^{1}TS(1-4)** the Bdan moiety is forced to be coplanar with the developing Ni···H bond, resulting in the extremely high energy of +56.3 kcal mol^{-1} (see ESI†).

Finally, alternative reactivity of the stable σ-borane complex **Int(1-4)1** was considered computationally.[43] One possibility involves IMes transfer to B which proceeds with a barrier of 14.8 kcal mol^{-1} to form a σ-B–H-bound adduct of HBdan–IMes at {Ni(IMes)} with an energy of +9.6 kcal mol^{-1}. From here reaction with a second equivalent of HBdan to give the dehydrocoupled product seen experimentally along with H_2 and the $[Ni(IMes)]_2$ dimer is computed to be thermodynamically favourable (G = −9.8 kcal mol^{-1}, see Fig. S25, ESI†).[44]

In summary, we report stark differences in the B–X bond activation chemistry of XBR_2 species (X = H or Cl, BR_2 = Bdan or Bcat) at $[Ni(IMes)_2]$, with the facile oxidative addition of B–Cl bonds contrasting the absence of any B–H activation. Computational studies relate these differences to the mechanism involved: B–Cl activation readily proceeds *via* nucleophilic displacement of Cl$^-$, while B–H activation would entail high energy – and hence inaccessible – concerted bond cleavage.

G. A. thanks the University of Surrey for a studentship. I. M. R. thanks the Royal Society of Chemistry for support (R21-1723146519). A. C. thanks Heriot-Watt University for a James Watt Scholarship. The authors thank Prof. Michael Whittlesey and Dr Mary Mahon for useful discussions.

Conflicts of interest

There are no conflicts to declare.

Notes and references

1 M. Wang and Z. Shi, *Chem. Rev.*, 2020, **120**, 7348.
2 J. Hu, M. Ferger, Z. Shi and T. B. Marder, *Chem. Soc. Rev.*, 2021, **50**, 13129.
3 N. Miyaura, *Comprehensive Organometallic Chemistry III*, Elsevier, 2007, vol. 9.
4 N. Miyaura, *Bull. Chem. Soc. Jpn.*, 2008, **81**, 1535.
5 G. J. Irvine, M. J. G. Lesley, T. B. Marder, N. C. Norman, C. R. Rice, E. G. Robins, W. R. Roper, G. R. Whittell and L. J. Wright, *Chem. Rev.*, 1998, **98**, 2685.
6 S. Aldridge and D. L. Coombs, *Coord. Chem. Rev.*, 2004, **248**, 535.
7 L. Dang, Z. Lin and T. B. Marder, *Chem. Commun.*, 2009, 3987.
8 U. Kaur, K. Saha, S. Gayen and S. Ghosh, *Coord. Chem. Rev.*, 2021, **446**, 214106.
9 S. J. Geier, C. M. Vogels, J. A. Melanson and S. A. Westcott, *Chem. Soc. Rev.*, 2022, **51**, 8877.
10 D. L. Kays and S. Aldridge, *Struct. Bond*, 2008, **130**, 29.
11 S. K. Bose, L. Mao, L. Kuehn, U. Radius, J. Nekvinda, W. L. Santos, S. A. Westcott, P. G. Steel and T. B. Marder, *Chem. Rev.*, 2021, **121**, 13238.
12 S. Manna, K. Kanti Das, S. Nandy, D. Aich, S. Paul and S. Panda, *Coord. Chem. Rev.*, 2021, **448**, 214165.
13 D. Adhikari, J. C. Huffman and D. J. Mindiola, *Chem. Commun.*, 2007, 4489.
14 T. P. Lin and J. C. Peters, *J. Am. Chem. Soc.*, 2014, **136**, 13672.
15 N. Curado, C. Maya, J. López-Serrano and A. Rodríguez, *Chem. Commun.*, 2014, **50**, 15718.
16 P. Ríos, J. Borge, F. Fernández, F. Fernández De Córdova, G. Sciortino, A. A. Lledós and A. Rodríguez, *Chem. Sci.*, 2021, **12**, 2540.
17 L. Tendera, F. Fantuzzi, T. B. Marder and U. Radius, *Chem. Sci.*, 2023, **14**, 2215.
18 L. Tendera, L. Kuehn, T. B. Marder and U. Radius, *Chem. – Eur. J.*, 2023, e202302310.
19 F. W. Seidel and K. Nozaki, *Angew. Chem., Int. Ed.*, 2022, **61**, e202111691.
20 H. Braunschweig, R. D. Dewhurst and A. Schneider, *Chem. Rev.*, 2010, **110**, 3924.
21 H. Braunschweig, P. Brenner, A. Müller, K. Radacki, D. Rais and K. Uttinger, *Chem. – Eur. J.*, 2007, **13**, 7171.
22 W. Clegg, F. J. Lawlor, G. Lesley, T. B. Marder, N. C. Norman, A. G. Orpen, M. J. Quayle, C. R. Rice, A. J. Scott and F. E. S. Souza, *J. Organomet. Chem.*, 1998, **550**, 183.
23 H. Braunschweig, P. Brenner, R. D. Dewhurst, F. Guethlein, J. O. C. Jimenez-Halla, K. Radacki, J. Wolf and L. Zöllner, *Chem. – Eur. J.*, 2012, **18**, 8605.
24 J. Zhu, Z. Lin and T. B. Marder, *Inorg. Chem.*, 2005, **44**, 9384.
25 S. Onozawa and M. Tanaka, *Organometallics*, 2001, **20**, 2956.
26 H. Braunschweig, K. Radacki, D. Rais and K. Uttinger, *Angew. Chem., Int. Ed.*, 2005, **45**, 162.
27 H. Braunschweig, H. Green, K. Radacki and K. Uttinger, *Dalton Trans.*, 2008, 3531.
28 H. Braunschweig, K. Gruss, K. Radacki and K. Uttinger, *Eur. J. Inorg. Chem.*, 2008, 1462.
29 F. Kong, P. Ríos, C. Hauck, F. J. Fernández-De-Córdova, D. A. Dickie, L. G. Habgood, A. Rodríguez and T. B. Gunnoe, *J. Am. Chem. Soc.*, 2023, **145**, 179.
30 L. Álvarez-Rodríguez, P. Ríos, C. J. Laglera-Gándara, A. Jurado, F. J. Fernández-de-Córdova, T. B. Gunnoe and A. Rodríguez, *Angew. Chem., Int. Ed.*, 2023, **62**, e202306315.
31 D. J. Nelson and F. Maseras, *Chem. Commun.*, 2018, **54**, 10646.
32 S. A. Westcott, H. P. Blom, T. B. Marder, R. T. Baker and J. C. Calabrese, *Inorg. Chem.*, 1993, **32**, 2175.
33 F. E. S. Souza, P. Nguyen, T. B. Marder, A. J. Scott and W. Clegg, *Inorg. Chim. Acta*, 2005, **358**, 1501.
34 R. B. Coapes, F. E. S. Souza, M. A. Fox, A. S. Batsanov, A. E. Goeta, D. S. Yufit, M. A. Leech, J. A. K. Howard, A. J. Scott, W. Clegg and T. B. Marder, *J. Chem. Soc., Dalton Trans.*, 2001, 1201.
35 C. M. Crudden and D. Edwards, *Eur. J. Org. Chem.*, 2003, 4695.
36 M. W. Kuntze-Fechner, H. Verplancke, L. Tendera, M. Diefenbach, I. Krummenacher, H. Braunschweig, T. B. Marder, M. C. Holthausen and U. Radius, *Chem. Sci.*, 2020, **11**, 11009.
37 L. Tendera, M. S. Luff, I. Krummenacher and U. Radius, *Eur. J. Inorg. Chem.*, 2022, e202200416.
38 N. A. Dodd, Y. Cao, J. Bacsa, E. C. Towles, T. G. Gray and J. P. Sadighi, *Inorg. Chem.*, 2022, **61**, 16317–16324.
39 A complementary situation pertains when the solvent correction was not included in the optimisation protocol, *i.e.* a transition state for concerted oxidative addition was characterised, but attempts to locate the nucleophilic displacement transition state failed (see Fig. S21–22, ESI†).
40 B–H activation *via* H atom transfer was also excluded (see Fig. S26, ESI†). The reactivity of XBCat (X = Cl, H) was also characterised computationally and gave similar results (see Fig. S21 and S22, ESI†).
41 I. Funes-Ardoiz, D. J. Nelson and F. Maseras, *Chem. – Eur. J.*, 2017, **23**, 16728.
42 L. Tendera, T. Schaub, M. J. Krahfuss, M. W. Kuntze-Fechner and U. Radius, *Eur. J. Inorg. Chem.*, 2020, 3194.
43 See Fig. S33–S35, ESI† for functional testing.
44 The details of the mechanism of this dehydrocoupling process were not pursued further, although the computed thermodynamics of N–H activation of HBdan at $[Ni(IMes)_2]$ ruled this process out (see Fig. S27, ESI†).

